JOURNAL OF MATERIALS SCIENCE 29 (1994) 3847–3856

# Load and directional effects on microhardness and estimation of toughness and brittleness for flux-grown $LaBO_3$ crystals

A. JAIN, A. K. RAZDAN, P. N. KOTRU
*Department of Physics, University of Jammu, Jammu 180001, India*
B. M. WANKLYN
*Department of Physics, Clarendon Laboratory, University of Oxford, Oxford OX1 3PU, UK*

Results of microhardness measurements on (1 0 0) and (1 1 0) planes of flux-grown $LaBO_3$ crystals, in the applied load range of 10–100 g, are presented. The microhardness was found to decrease with increasing load in a non-linear manner. By applying Hays and Kendall's law, the materials resistance pressure and other constants of the equation could be calculated. Hardness anisotropy, showing periodic variation of $H_v$ with the maxima and minima repeating at every 15° change in orientation of the indentor, is described and discussed. $H_{max}/H_{min}$ are estimated as 1.14 and 1.06 for (1 0 0) and (1 1 0) planes, respectively. The fracture toughness values, $K_c$, determined from measurements of crack lengths, are estimated to be 1.6, 1.7 $MN\,m^{-3/2}$ (for (1 0 0) planes) and 1.2, 1.5 $MN\,m^{-3/2}$ (for (1 1 0) planes) at 90 and 100 g loads, respectively. The brittleness index, $B_i$, is estimated as 4.6, 4.0 $\mu m^{-1/2}$ (for (1 0 0) planes) 6.0, 4.6 $\mu m^{-1/2}$ (for (1 1 0) planes) at 90 and 100 g, loads respectively.

## 1. Introduction

Indentation-induced hardness testing studies provide useful information concerning the mechanical behaviour of materials. It was found by Buckle [1] that various material properties can be investigated using microhardness measurements. The microscopic hardness indentations are made with very small loads and they are used to investigate local hardness variations in single-phase and multiphase materials. The determination of a materials hardness is normally made using the mechanical test that gives a measure of ease with which the material can locally be deformed; usually an indentation or scratch test is performed under defined conditions. The size of the indentation or scratch is related to the applied load and yield stress of the materials [2]. Most hardness tests produce plastic deformation in materials and all variables which affect plastic deformation affect hardness [3]. The ability of the material to resist permanent deformation is usually considered to be the definition of hardness.

There are many reports of Vicker's microhardness measurements on various crystals [4–31]. The dependence of Vicker's microhardness, $H_v$, on applied load shows a different behaviour for different materials. The variation of microhardness with increasing load may be classified into four types.

(i) $H_v$ remains unaffected [19];
(ii) $H_v$ decreases [4, 5, 17, 27, 29, 30];
(iii) $H_v$ increases [28]; and
(iv) $H_v$ shows complex variation [7–9,15,21,23–25,31].

Various laws have been suggested to explain the variation of microhardness with load. Kick's law [32] ($P = K_1 d^n$) postulates $n = 2$ which, however, should apply under the conditions where the measured hardness is truly independent of the load. The concept of Onitsch [33] is that if $n > 2$, the microhardness number increases as the load is increased. $n$ is almost invariably significantly less than 2 [34] particularly for hard ceramic materials. Considering the sample resistance pressure, Hays and Kendall [35] have suggested an equation $P - W = K_2 d^n$ where $n = 2$ (the definition of terms used here is given later in the text).

Another significant problem is the hardness anisotropy. Effect of crystal orientation on hardness of crystals has been studied by a number of workers [26, 36–43]. To the best of our knowledge, anisotropy of microhardness has not so far been reported on lanthanum borates. In this paper, the results on anisotropy of the Vicker's microhardness are presented on the basis of measurements taken on two different planes, (1 0 0) and (1 1 0), with different orientation of each crystal plane with respect to the indentor.

In order to make comparative studies of microhardness with load and hardness anisotropy on two different planes, the authors undertook measurements of hardness on (1 0 0) and (1 1 0) faces of the same crystal of $LaBO_3$.

## 2. Experimental procedure

$LaBO_3$ has the orthorhombic structure of argonite and is pseudo-hexagonal, with the pseudo-hexagonal $c$-axis parallel to the orthorhombic $b$-axis [44–46]. $LaBO_3$ crystals considered here were grown using the flux technique as reported by Kotru and Wanklyn [47]. The

0022–2461 

crystals were in the form of plates ($10 \times 3 \times 1$ mm$^3$), rods ($4 \times 1.5 \times 1$ mm$^3$) and tabular ($4 \times 3 \times 1$ mm$^3$).

These crystals do not exhibit perfect cleavage and therefore plane habit faces free from any scratches were chosen for the indentation purposes. Selected (1 0 0) and (1 1 0) plane surfaces were used for microhardness measurements at room temperature (30 °C), using a Vicker's microhardness tester mhp 100 attached to the metallurgical microscope Neophot-2, manufactured by Carl Zeiss, Germany. Loads ranging from 10–100 g were used for indenting samples, keeping the indentation time at 10 s. $H_v$ was calculated using the equation $H_v = (1.8544\, P/d^2)\ 10^3\ \mathrm{kg\,mm^{-2}}$, where $P$ is the load applied (g), and $d$ is the diagonal length of the indentation impression (μm). In our experiments, the measurements of the diagonal length are taken on ten indentations for a particular load and for each indentor impression, the diagonal length is taken as the average of the two diagonals. In other words, the value of $d$ for each load is essentially an average of 20 measurements.

Considering the formula for microhardness $H_v = 1.8544\ p/d^2$ the standard error on $P$ and mean values of $d$ were calculated. Thus the errors on $H_v$ were estimated for each $P/d^2$ using the formula

$$\Delta H_v = 1854.4\,[\{(1/y)\Delta P\}^2 + P^2/y^4(\Delta y)^2]^{1/2} \quad (1)$$

where $y = d^2$, $\Delta y = 2\,d\Delta d$, $\Delta P$ is the experimental error on $P$.

Computational errors were also estimated for quantities such as log $P$, $d$, $K$, $W$ and log $(P - W)$. The data were plotted by the least square fit method by feeding the data into a Vax 11/730 manufactured by DEC America.

## 3. Results and discussion

### 3.1. Indentation of (1 0 0) and (1 1 0) planes

For plastically yielding materials, the size of the indentation is related to the applied load and the yield stress. Although dislocation generation is evident in the deformed zone beneath an indentation [48], deformation may not generally be accommodated without some measure of cracking. An exception may be under very low loads where the strain energy is insufficient to nucleate cracks [49]. In most cases, cracking occurred.

Figs 1a, c and 2a, c show indentations on application of 90 and 100 g loads, respectively, on (1 0 0) and (1 1 0) faces of an $LaBO_3$ crystal. Figs 1b, d and 2b, d are the corresponding etch patterns on the indented impressions of Figs 1a, c and 2a, c, respectively. The defect structure created as a result of indentation is indicated by the result of etch patterns around the site of indentation when the crystal is etched in 90% $HNO_3$ for 1 h at room temperature (30 °C). In all these cases, the indentations were made with different loads keeping one of the diagonals of the Vicker's indentor parallel to a $\langle 0\,0\,1 \rangle$ direction (i.e. parallel to the edges of intersection of $\{1\,0\,0\}$ and $\{1\,1\,0\}$ faces) on the (1 0 0) surface. Similarly, on (1 1 0) surfaces, one of the diagonals of the Vicker's indentor was kept parallel to a $\langle 0\,0\,1 \rangle$ direction (i.e. $\{1\,1\,0\}$–$\{1\,0\,0\}$ edge). As is quite evident in these figures, indentation of the sample has led to straight and radial cracks. This clearly reveals that the etch figure star around the indentation indicating the interaction of dislocations around the slip traces (as, for example, observed in the case of other crystals [6]), is not formed in this case. The dark lines (due to heavy preferential etching along them), originating from the indentation marks in different directions, are cracks produced due to rupture.

### 3.2. Variation of $H_v$ with load

The Vicker's microhardness values as measured on (1 0 0) and (1 1 0) faces of an $LaBO_3$ crystal in the load range 10–100 g are given in Table I. The variation of $H_v$ with load is judged from the curves recorded in Fig. 3, which reveal a non-linear relationship between microhardness and the applied load, irrespective of whether the plane considered is (1 0 0) or (1 1 0). The variation of $H_v$ with load is similar for the two planes. It is also significant to note that this behaviour is similar to those of other materials as reported in the literature published from this laboratory [27, 29, 30].

According to Kick's law [32] the dependence of microhardness on indentation length (and hence $H_v$ on load) is given by the equation

$$P = K_1\, d^n \quad (2)$$

where $P$ is the applied load, $d$ the length of the indentation diagonal, $K_1$ the material constant (standard hardness) and $n$ is the Meyer index. This equation can be considered as an established one only if it explains the variation of $H_v$ with load. The value of $n$ is an important factor in validating the application of this equation. The often-quoted value of $n = 2$, is true for conditions where the measured hardness is truly independent of the load. However, this is not so in either the present case or the cases reported by other authors [2, 7, 27, 29, 30, 33, 50–61]. Brookes [34] has reported that $n$ is almost invariably significantly less than 2. The detailed work of Burnand [38] and Ross [62] established that consistent values of $n < 2$ were obtained irrespective of specimen surface preparations (cleaved or chemically polished) and whether or not the crystals (LiF and MgO) were immersed in a selection of electrolytes. The possibility of an explanation of $n$ always being less than 2 based on surface characteristics and such environmental conditions as those associated with Rebinder-type effects, were ruled out by the detailed work of these authors. Values of $n < 2$ have also been reported to have remained reasonably constant for silicon and germanium when indented at temperatures up to 573 K [62].

It is interesting to determine the values of $n$ from the data as recorded in Table I for flux-grown $LaBO_3$ crystals. Based on the application of Kick's equation ($P = K_1\, d^n$), the curve log $P$ versus log $d$ should yield a straight line with a slope giving the value of $n$ (Fig. 4a). Here, the slope gives the value of $n < 2$ for both the planes (see Table II).

Hays and Kendall [32] have modified Kick's law to the equation

$$P - W = K_2 d^2 \quad (3)$$

where $K$ is a constant, $n = 2$ is the logarithmic index and $W$ is the resistance pressure and represents the minimum applied load to cause an indentation, as

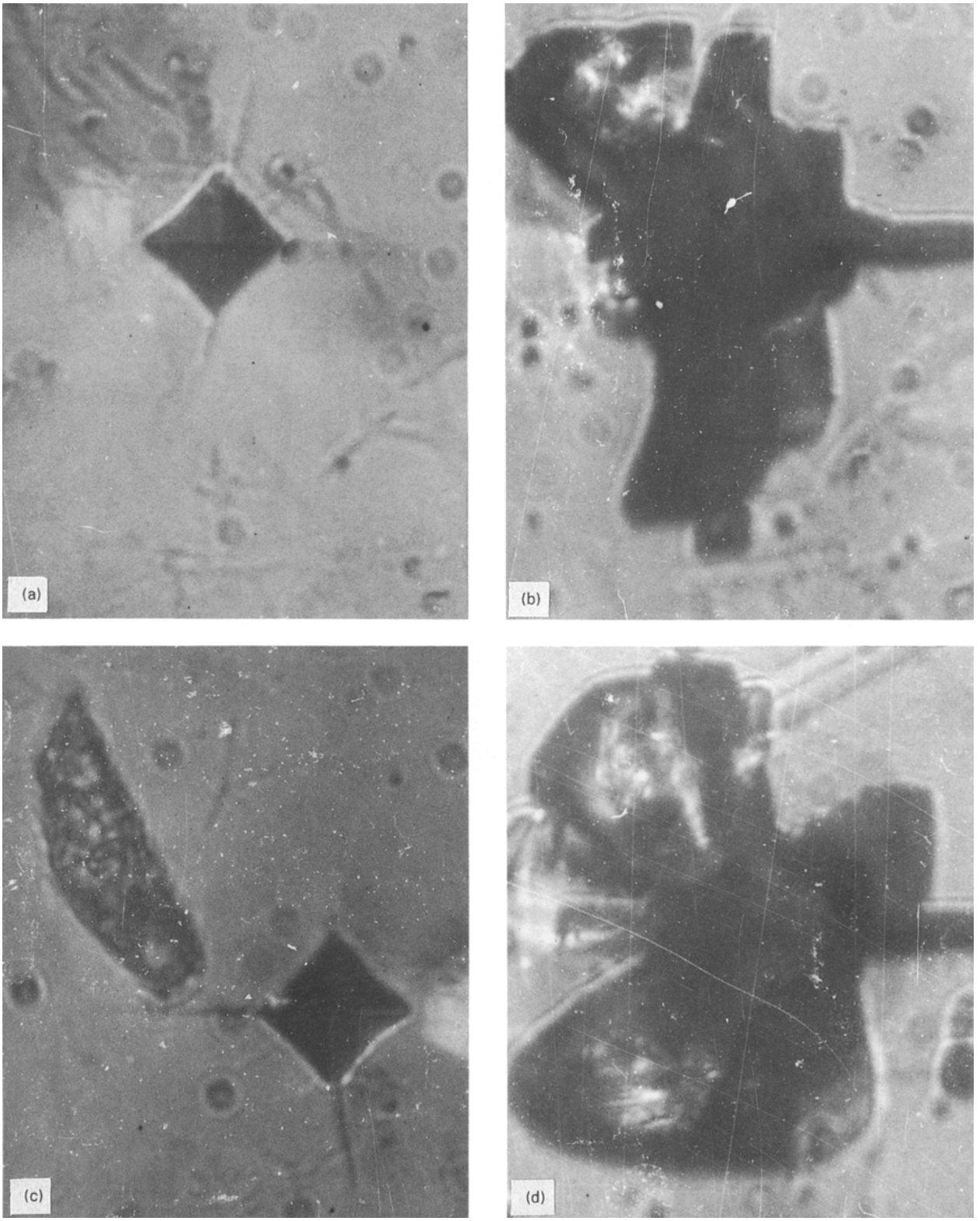


*Figure 1* (a, c) Indentation impressions on the (1 0 0) face on application of (a) 90 g and (c) 100 g load. (b, d) Corresponding etch patterns of (a) and (c), respectively, after etching in 90% $HNO_3$ at 30 °C for 1 h. × 500.

loads less then $W$ will, by definition, allow no plastic deformation. The function $W$ may be evaluated for a particular solution on solving the two equations (Kick's and Hays' and Kendall's laws) by subtraction. Thus

$$W = K_1 d^n - K_2 d^2 \quad (4)$$

or

$$d^n = W/K_1 + K_2/K_1 d^2 \quad (5)$$

The evaluation can now be completed by simple graphical methods, i.e. a plot of log $P$ versus log $d$ gives the value of $n$ and $K_1$ for the two planes (see Fig. 4a and Table II) and $n < 2$ for both the planes. A Cartesian plot of Equation 5, for $d^n$ versus $d^2$ yields the slope $K_2/K_1$ and the intercept $W/K_1$ (Fig. 5). The values obtained are also recorded in Table II, which thus gives compiled data of all the factors required for the application of Hays' and Kendal's law.

Fig. 4b, a plot of log $(P - W)$ versus log $d$, yields a straight line, the slope of which gives the value of

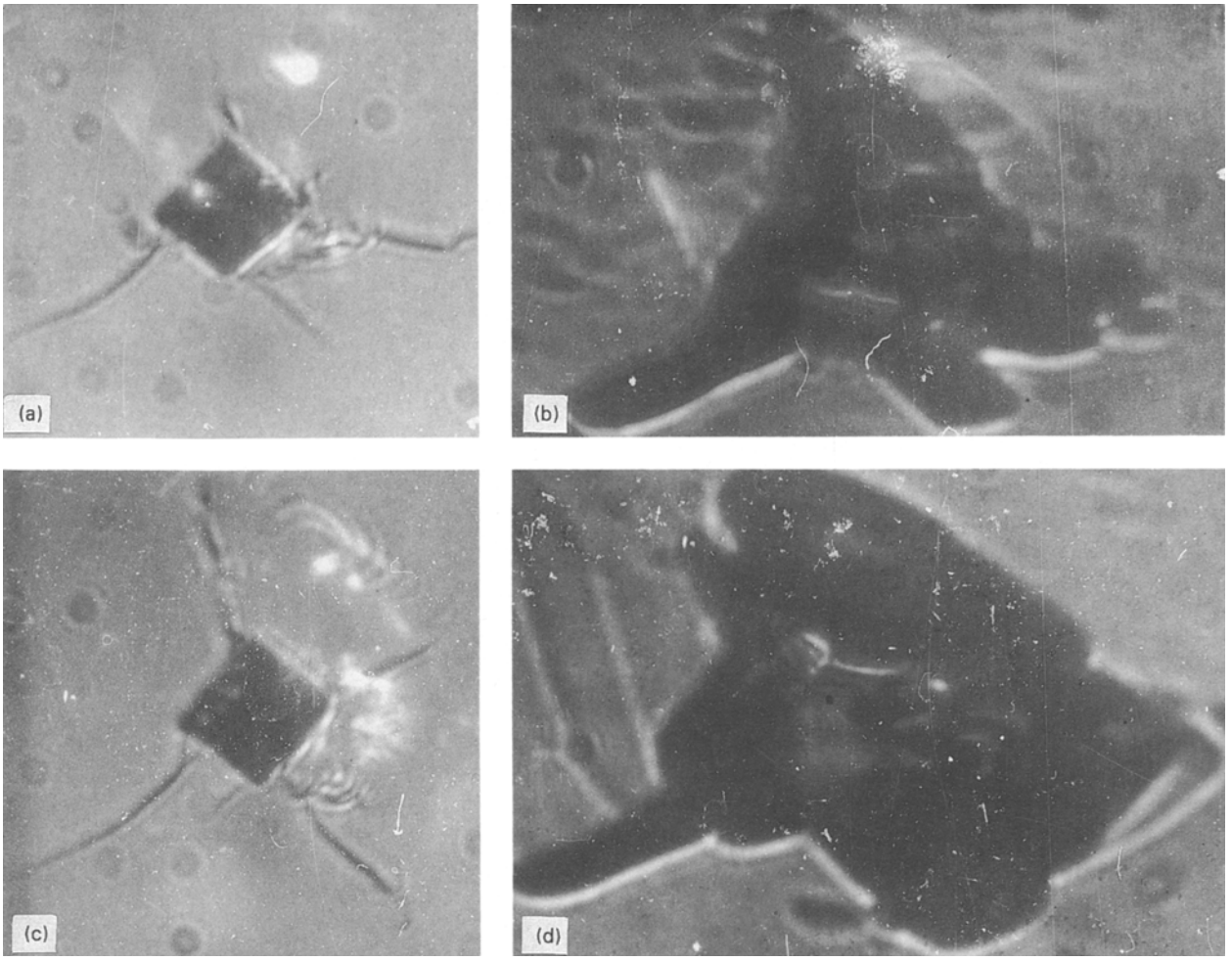


*Figure 2* (a, c) Indentation impressions on the (110) face on application of (a) 90 g and (b) 100 g load. (b, d) Corresponding etch patterns of (a) and (c), respectively, after etching in 90% $HNO_3$ at 30 °C for 1 h. × 500

TABLE I Vicker's hardness number at different loads on (1 0 0) and (1 1 0) faces of $LaBO_3$ crystal

| $P$ (g) | $H_v$ | | Difference in hardness value (kg mm$^{-2}$) |
|---|---|---|---|
| | (1 0 0) face (kg mm$^{-2}$) | (1 1 0) face (kg mm$^{-2}$) | |
| 10 | 903 | 997 | 94 |
| 20 | 861 | 931 | 70 |
| 30 | 849 | 919 | 70 |
| 40 | 833 | 891 | 58 |
| 50 | 821 | 867 | 46 |
| 70 | 795 | 852 | 57 |
| 80 | 778 | 778 | 0 |
| 90 | 736 | 730 | 6 |
| 100 | 697 | 689 | 8 |

$n = 2$, whether the plane considered is (1 0 0) or (1 1 0). It is thus concluded that

(i) the material considered falls in the class for which the concepts of a materials resistance pressure as proposed by the Hays and Kendall [35] law is applicable;

(ii) the above concept is valid whether the planes considered are (1 0 0) or (1 1 0).

## 3.3. Orientation dependence of $H_v$

It is well known that the capacity of a crystal to deform plastically is a directional or anisotropic property. Because indentation hardness involves plastic deformation, one can foresee that such hardness may be a function of the orientation of the indented crystal.

A definite indication of directional hardness of minerals using the Knoop indentor has been reported

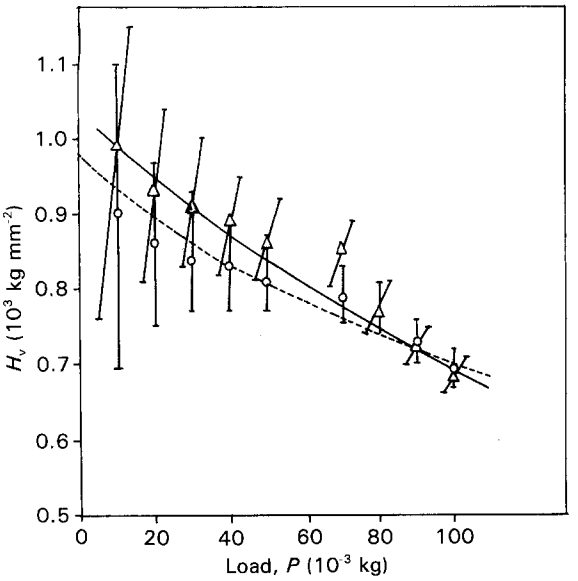


*Figure 3* The dependence of microhardness on load on (– – –) (1 0 0) and (——) (1 1 0) faces.

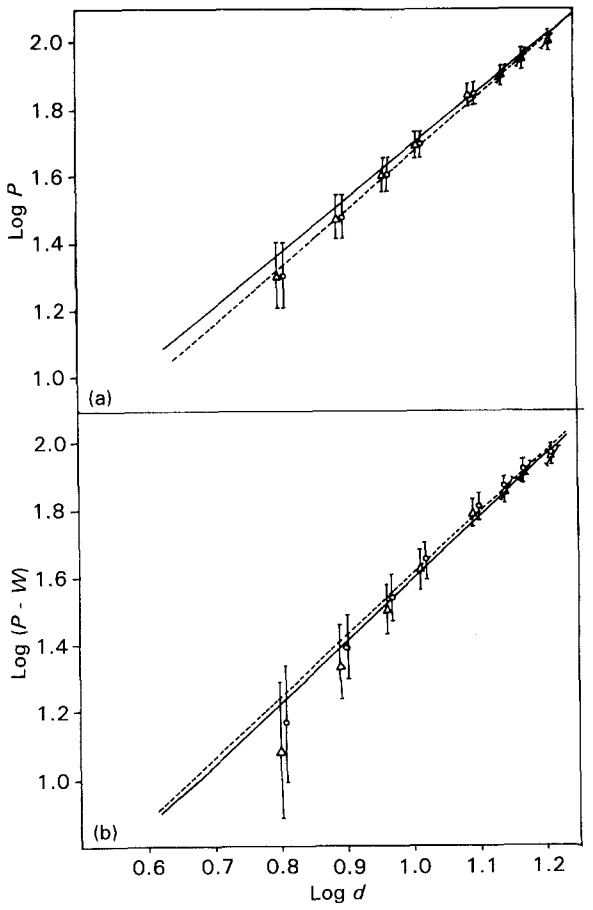


*Figure 4* (a) Log $P$ versus log $d$ and (b) log $(P-W)$ versus log $d$, for (– – –) (1 0 0) and (——) (1 1 0) faces.

TABLE II Results of hardness analysis of $LaBO_3$ crystals on (1 0 0) and (1 1 0) faces

| Face | $n$ | $K_1$ ($10^3$ kg mm$^{-2}$) | $K_2$ ($10^3$ kg mm$^{-2}$) | $W/K_1$ ($10^{-6}$ mm$^2$) | $W$ ($10^{-3}$ kg) |
|---|---|---|---|---|---|
| (1 0 0) | 1.70764 | 0.8752 | 0.3765 | 5.9192 | 5.1805 |
| (1 1 0) | 1.58768 | 1.2127 | 0.3678 | 6.3757 | 7.7322 |

[53, 65]. Also Daniel and Dunn [36] reported periodic variation of hardness with orientation of the Knoop indentor with respect to the metallic crystals. Orientation dependence of indentation hardness has also been reported by Shah [26], using the Vicker's indentor.

In order to study the effect of crystal orientation on the Vickers hardness of single crystals of $LaBO_3$, the measurements converted to Vickers hardness number, $H_v$, were plotted against angular displacement of the Vickers indentor from the 0° index line. The initial position (0°), was taken when one of the diagonals of the indentor on the (1 0 0) face was parallel to a ⟨0 0 1⟩ direction. The same applies to the measurements on (1 1 0) planes. Measurements were taken after every 15° angular displacement of the indentor loaded with 50 g. A load of 50 g was chosen in order to obtain the optimum size of the indentation mark as suggested by Buckle [66]. Results for (1 0 0) and (1 1 0) planes of $LaBO_3$ crystal are shown later in Fig. 10.

Fig. 6a–c illustrate the indented impressions at 50 g load and the associated straight and radially curved crack patterns on the (1 0 0) face corresponding to 0°, 90° and 135° orientation of the indentor. Fig. 7a–c are the corresponding etch patterns revealing the deformation patterns around the indented regions of Fig. 6a–c. No such etch features are observed for any orientation of the indentor (angular displacement of 0°–180° in steps of 15°), which could be attributed to slip traces. However, deformation has occurred around the indentation which has resulted in cracks, irrespective of orientation of the indentor. The deformation around the indentation at orientations of 0°, 90° and 135° of the indentor for (1 0 0) faces are illustrated as examples. The deformation around the indentation is revealed by etch patterns around the indented regions (e.g. see Fig. 7a–c).

Fig. 8a–c illustrate the indentation impressions at the same load of 50 g on the (1 1 0) face, keeping the orientation of the indentor at 0°, 90° and 135° with respect to the index line as already explained. Here

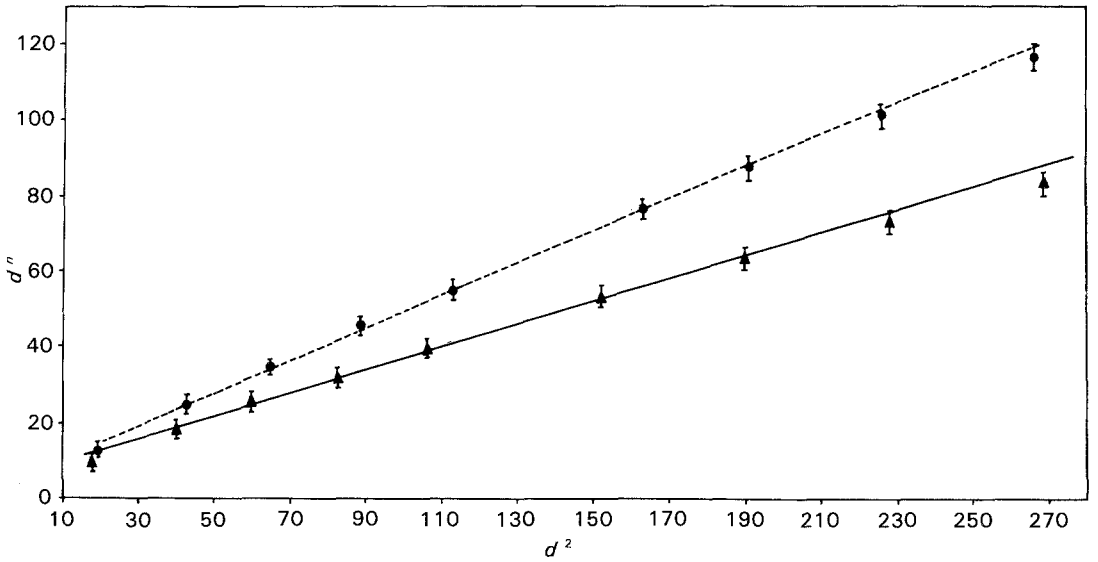


*Figure 5* A plot of $d^n$ versus $d^2$ for (– – –) (1 0 0) and (——) (1 1 0) faces of $LaBO_3$ crystals.

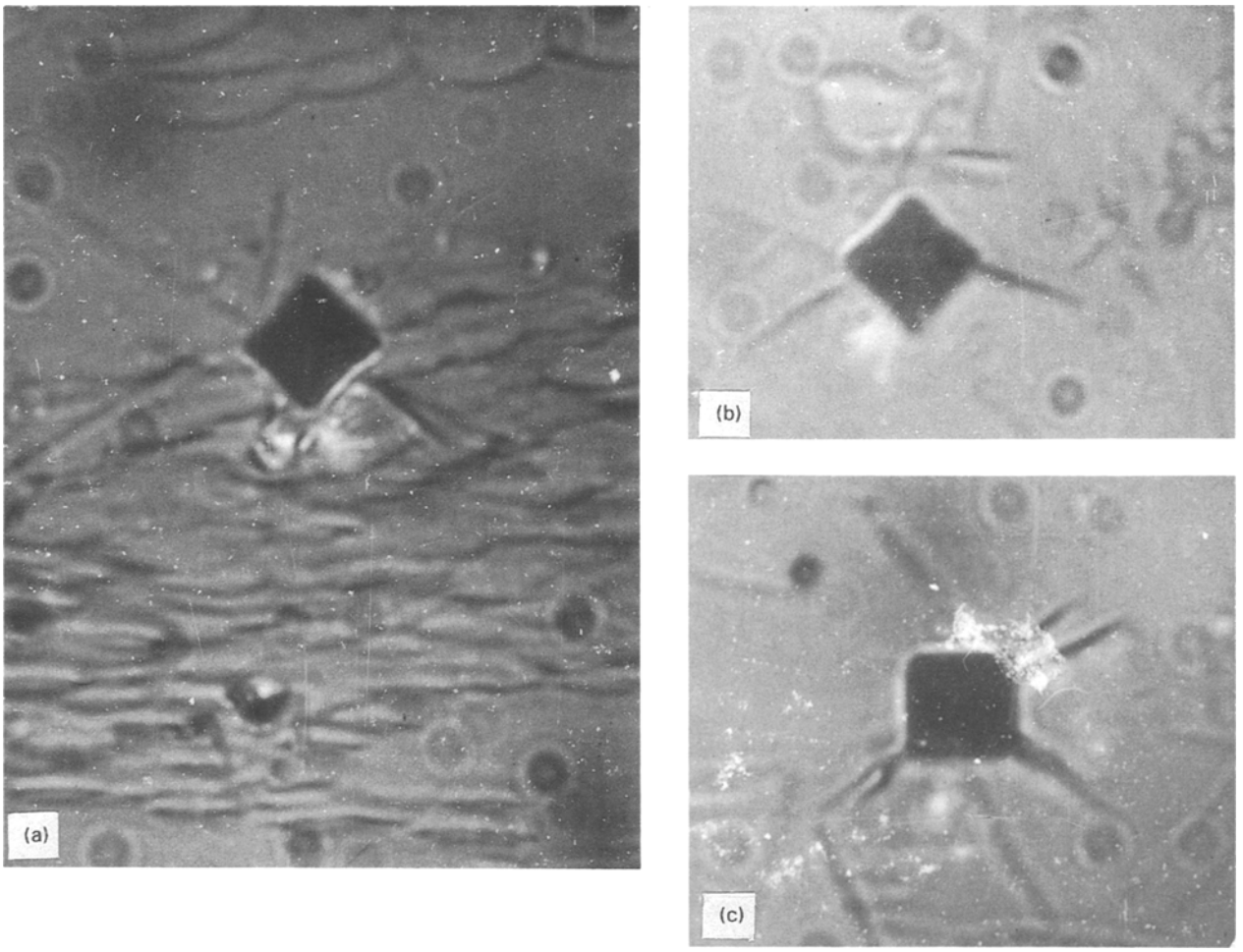


*Figure 6* Indentation impressions at 50 g load on the (1 0 0) face corresponding to (a) 0°, (b) 90° and (c) 135° angular displacements with respect to the initial setting. × 500

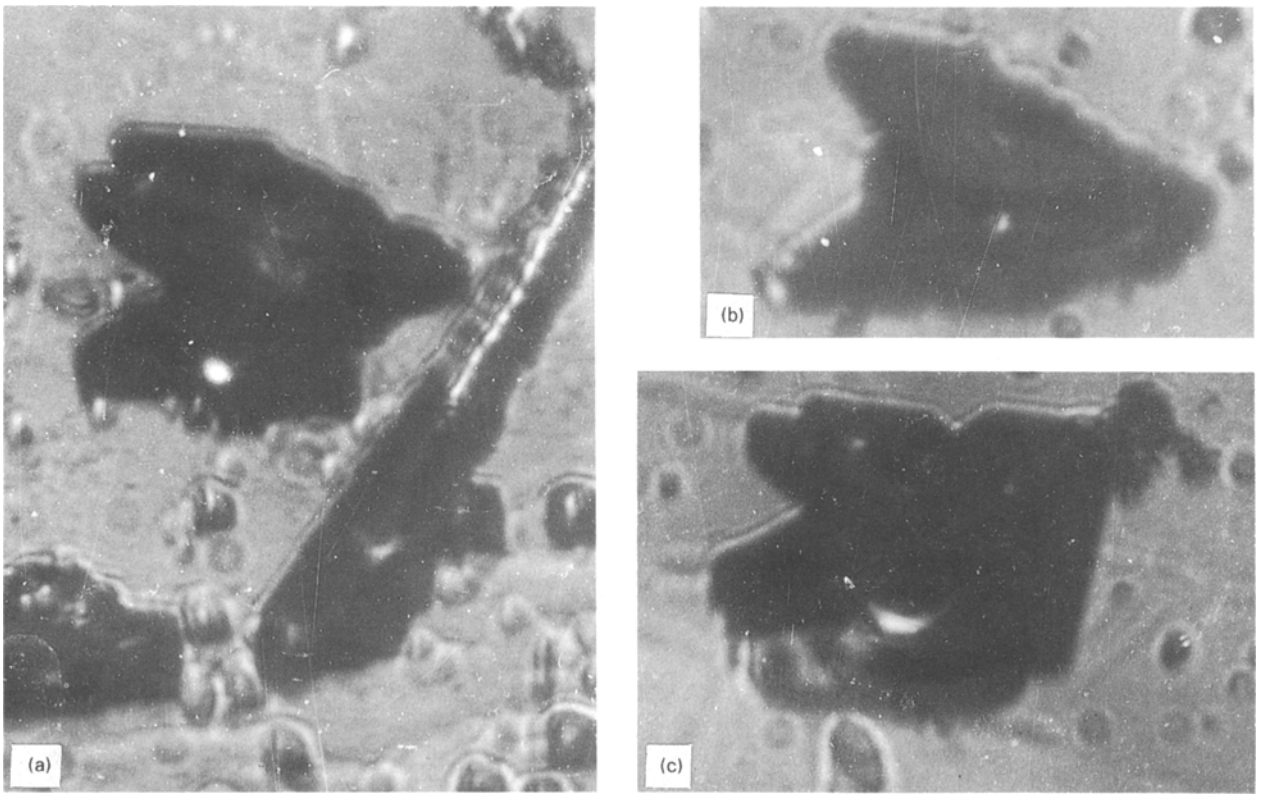


*Figure 7* (a–c) Corresponding etch patterns around the indented regions of Fig. 6a–c after etching in 90% $HNO_3$ at 30°C. × 500.

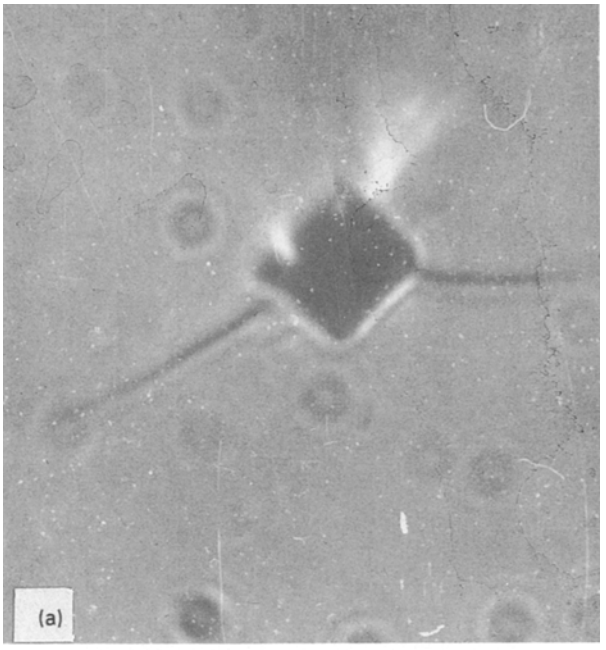


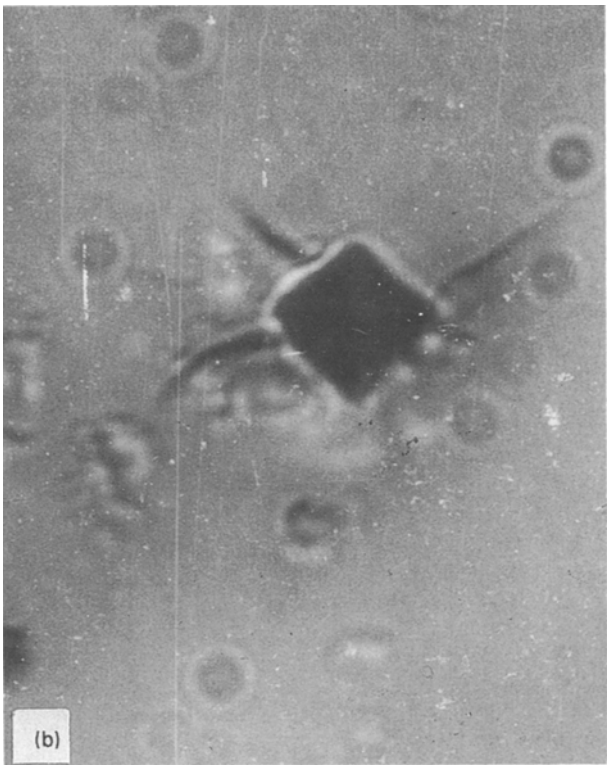


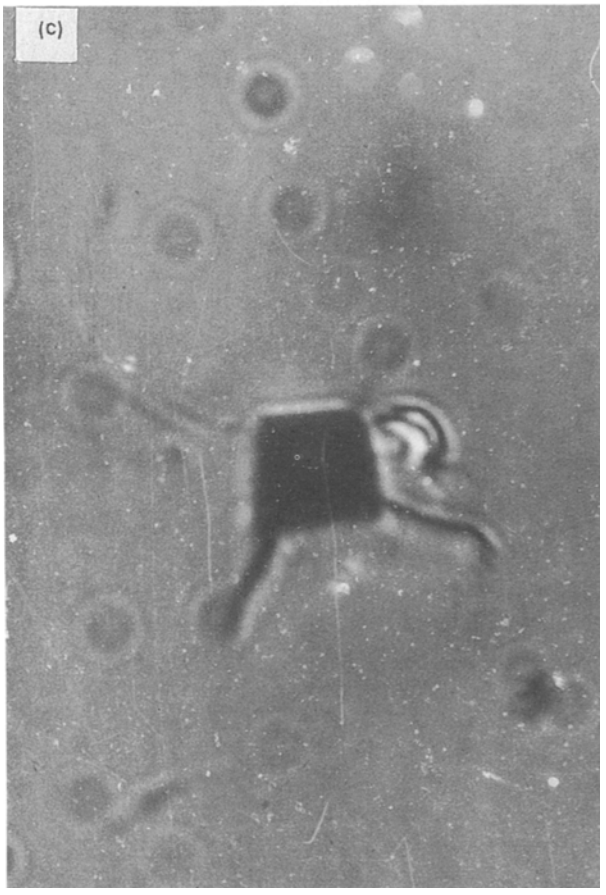


*Figure 8* Indented impression at 50 g load on the (1 1 0) face of an $LaBO_3$ crystal corresponding to (a) 0°, (b) 90° and (c) 135° angular displacement with respect to the initial setting. × 500

also the cracks develop at all the orientations of the indentor. Fig. 9a–c show the corresponding etch patterns obtained on indented samples of Fig. 8a–c. Here also the etch patterns do not reveal the creation of slip traces as a result of indentation. Only straight and radially curved cracks are observed at all orientations of the indentor. The deformation around the indented area is indicated by the etch patterns of Fig. 9a–c corresponding to indented regions of Fig. 8a–c.

Because the hardness number is defined in terms of the size of the indentor impression, any anisotropic effect shown by the size of the indentation mark on the given specimen will affect the hardness results obtained. In order to study the anisotropy exhibited by (1 0 0) and (1 1 0) planes of the $LaBO_3$ crystals, directional hardness was determined by rotation of the indentor over a range of 0°–180° in stages of 15°.

The values of Vicker's microhardness for both the faces are given in Table III and the pattern of variations is recorded in Fig. 10. From the graphs the following points emerge.

(i) Whether the planes considered are (1 0 0) or (1 1 0), the variation is periodic, the maxima and minima repeating at every 30° change in orientation.

(ii) At the initial setting (0°) the minimum of a (1 0 0) plane corresponds to the maximum of a (1 1 0) plane.

(iii) The maximum value on the (1 0 0) plane is more than the maximum value on the (1 1 0) plane, whereas the minimum has the same value on both the planes (i.e. (1 0 0) and (1 1 0)).

(iv) The ratio between the two extreme values of hardness, i.e. $H_{max}/H_{min}$, is 1.14 and 1.06 for (1 0 0) and (1 1 0) planes, respectively. Here $H_{max}$ is the microhardness value of the crystal for 15°, 45°, 75°, etc., and 0°, 30°, 60°, etc., orientation of the indentor with reference to its initial setting for (1 0 0) and (1 1 0) planes, respectively.

The above results indicate the anisotropic behaviour of microhardness for $LaBO_3$ crystals.

The slip system and the crystal structure play a primary role in the observed variation of directional

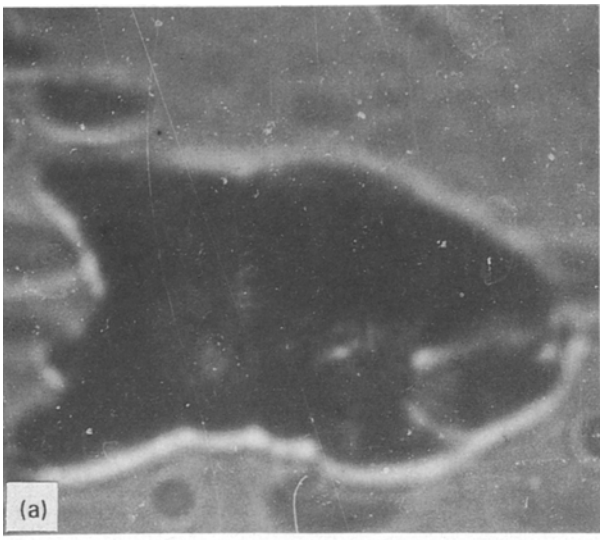


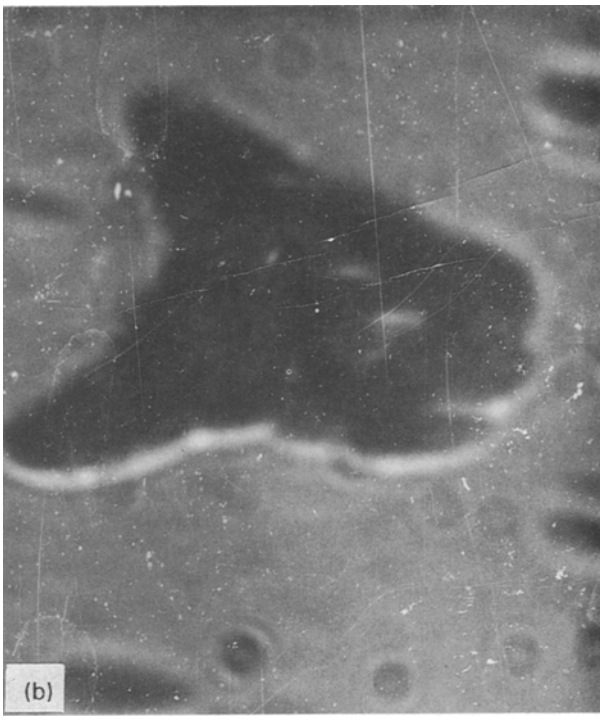


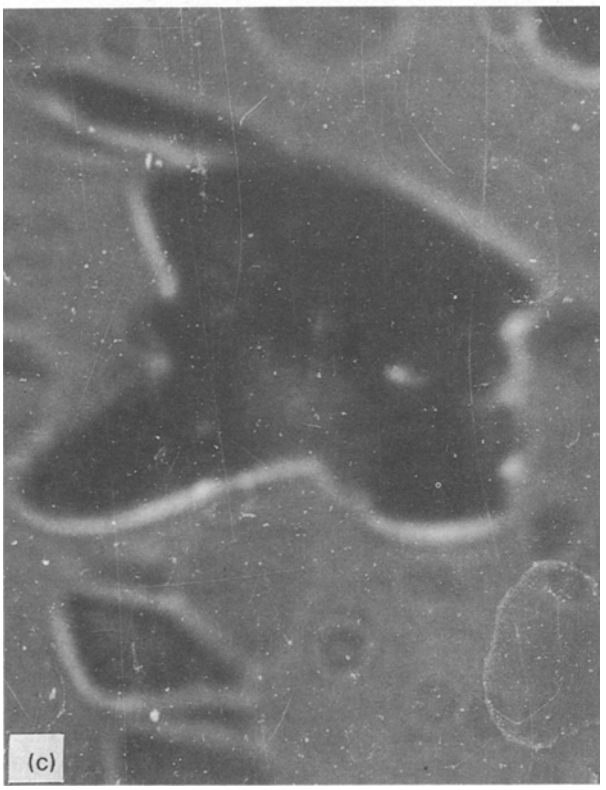


*Figure 9* (a–c) Corresponding etch patterns around the indented regions of Fig. 8a–c after etching in 90% $HNO_3$ at 30 °C for 1 h. × 500

TABLE III Variation of directional hardness on (1 0 0) and (1 1 0) faces of $LaBO_3$ crystals. Applied load = 50 g, indentation time = 10 s

| Orientation w.r.t. first setting (deg.) | $H_v$ (kg mm$^{-2}$) | |
|---|---|---|
| | (1 0 0) face | (1 1 0) face |
| 0 | 841 | 733 |
| 15 | 733 | 784 |
| 30 | 841 | 733 |
| 45 | 733 | 784 |
| 60 | 841 | 733 |
| 75 | 733 | 784 |
| 90 | 841 | 733 |
| 105 | 733 | 784 |
| 120 | 841 | 733 |
| 135 | 733 | 784 |
| 150 | 841 | 733 |
| 165 | 733 | 784 |
| 180 | 841 | 733 |

hardness as well as in the observed variation of hardness with load. The size of the indentation mark can be regarded as a measure of the ease of slip, a larger indentation appearing when the resolved shear stress is high and a smaller indentation when it is low. When the slip plane is suitably oriented, the yield stress is minimum. Thus the directional variation in hardness is due to the change in orientation of the indentor with respect to the active slip system of the crystal, as has also been reported by Shah [26].

That the hardness value is repeated after every 30° indicates that the crystal may have 12-fold symmetry. In fact, it must be considered that the measuring instrument, namely the Vicker's indentor, has four-fold symmetry which repeats the value of $H_v$ after every 90° rotation. This suggests that there is a manifestation of three-fold symmetry as far as the anisotropy property of microhardness is concerned.

## 3.4. Fracture toughness and brittleness

The indentor impressions are seen here in association with cracks at all loads, whether the planes considered are (1 0 0) or (1 1 0).

Resistance to fracture indicates the toughness of a material. For a solid containing a well-developed crack, fracture toughness, $K_c$, determines the fracture

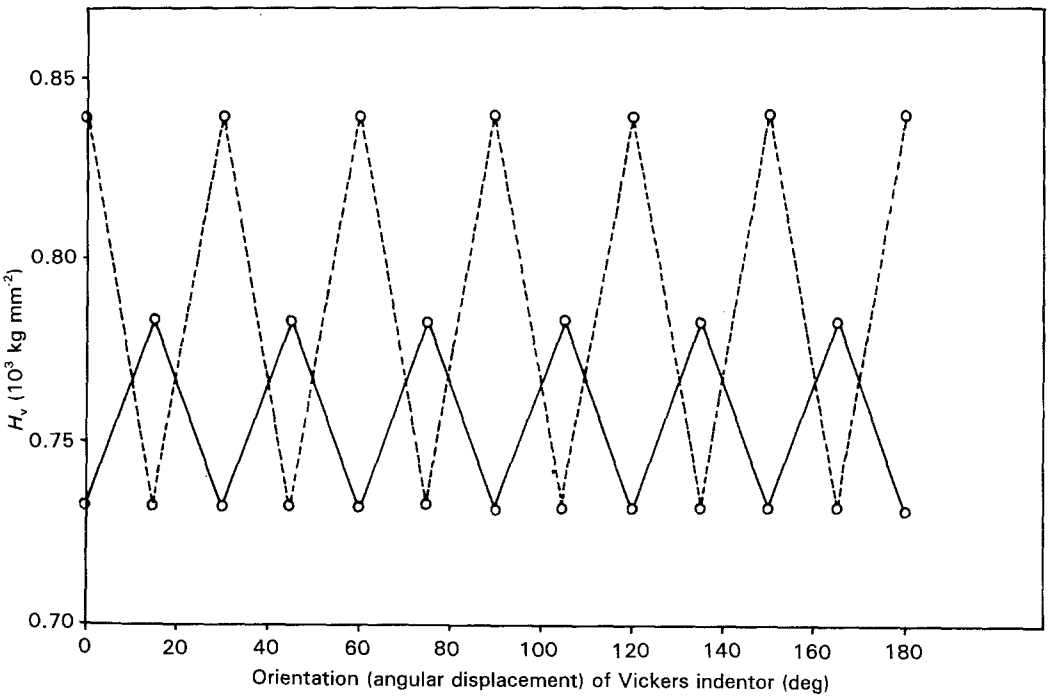


*Figure 10* $H_v$ versus orientation (angular displacement) of the indentor for (– – –) (1 0 0) and (——) (1 1 0) faces, indicating periodic variations.

stress on uniform tensile loading. The fracture mechanics of the indentation process gives an equilibrium relation for a well-developed crack extending under centre-loading conditions

$$P/l^{3/2} = B_0 K_c \qquad l \geqslant d/2 \tag{6}$$

where $P$ is the applied load (kg) and $l$ is the crack length measured from the centre of the indentation mark to the crack end. It may be noted that only well-defined cracks have been considered and the crack length, $l$, is the average of the two crack lengths for each indentation. $B$ is the indentor constant, taken as 7 for the Vickers indentor [67].

It is well known that the fracture strength of solids is related to their hardness and fracture toughness [68, 69]. The value of fracture toughness, $K_c$, as determined from the measurements of crack lengths, was estimated to be 1.6, 1.7 MN m$^{-3/2}$ (for (1 0 0) planes) and 1.2, 1.5 MN m$^{-3/2}$ (for (1 1 0) planes) at 90 and 100 g load, respectively.

Fig. 11 illustrates the variation of crack length $l$ and $H_v$ for the (1 1 0) face. Because, in the case of the material considered, $H_v$ varies with load, it is clear that the crack length would also depend on the applied load. (The dependence of crack length on $H_v$ and load is shown in Fig. 11.)

Brittleness is an important property which is expressed in terms of the brittleness index, $B_i$, defined as

$$B_i = H_v/K_c \tag{7}$$

It is estimated to be 4.6, 4.0 μm$^{-1/2}$ (for (1 0 0) planes) and 6.0, 4.0 μm$^{-1/2}$ (for (1 1 0) planes) at 90 and 100 g loads, respectively.

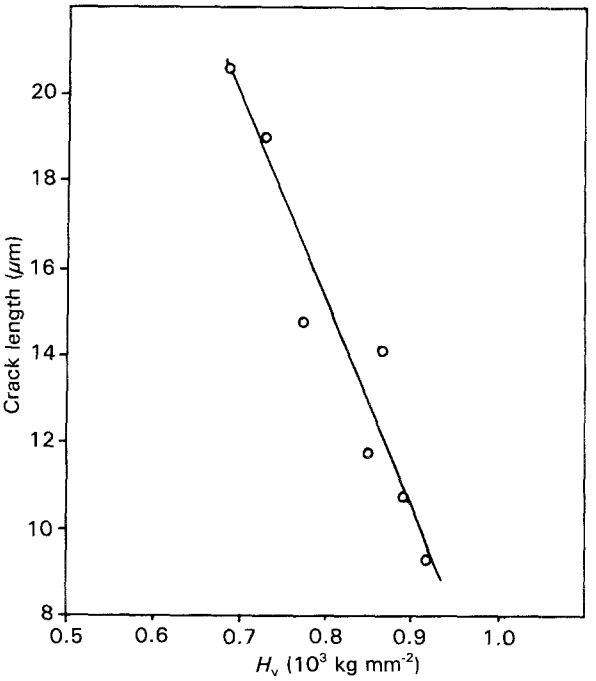


*Figure 11* Crack length versus $H_v$ for the (1 1 0) face.

## 4. Conclusions

1. The Vicker's microhardness value, $H_v$, of flux-grown $LaBO_3$ is in the range 903–697 kg mm$^{-2}$ for (1 0 0) planes and 997–689 kg mm$^{-2}$ for (1 1 0) planes, under the application of load in the range 10–100 g. The variation of $H_v$ with load is non-linear irrespective of whether the planes considered are (1 0 0) or (1 1 0). The microhardness value decreases as the load increases.

2. The variation of $H_v$ with load does not obey Kick's law (where $n = 2$). Instead, the hardness data fit in very well with the application of Hays and Kendall's law [35] ($P - W = K_2 d^2$) suggesting thereby that the concept of a materials resistance pressure is applicable in this case also whether the planes considered are (1 0 0) or (1 1 0).

3. The hardness is a function of the orientation of the indented $LaBO_3$ crystals, thus exhibiting the anisotropic property. Whether the planes considered are (1 0 0) or (1 1 0) the variation is periodic, the maxima

and minima are repeated every 30° change in orientation. At 0°, the minimum has the same value on both the planes ((1 0 0) and (1 1 0)); the ratio between the two extreme values of hardness, i.e. $H_{max}/H_{min}$, being 1.14 and 1.06 for (1 0 0) and (1 1 0) planes, respectively.

4. The fracture toughness value, $K_c$, is estimated to be 1.6, 1.7 $MN m^{-3/2}$ for (1 0 0 planes) and 1.2, 1.5 $MN m^{-3/2}$ (for 1 1 0) planes at 90 and 100 g loads, respectively.

5. The brittleness index, $B_i$, is estimated as 4.6, 4.0 $\mu m^{-1/2}$ (for 1 0 0 planes) and 6.0, 4.6 $\mu m^{-1/2}$ (for 1 1 0 planes) at 90 and 100 g, respectively.

## Acknowledgement

One of the authors (A.J.) thanks the University Authorities for the award of a University Research Fellowship.

## References

1. H. BUCKLE, *Mater Rev.* **4** (1959) 49.
2. D. J. CLINTON and R. MORRELL, *Mater. Chem. Phys.* **17** (1987) 461.
3. W. HAYDEN, N. G. MOFFATT and J. WULFF, 'The Structure and Properties of Materials', Vol. III, Mechanical Behaviour (Wiley Eastern, New York, 1968).
4. H. BUCKIE, "Progress in microindentation hardness testing" (Victor petterson Bukindustriak tiboday, Stockholm, 1945).
5. G. P. UPIT and S. A. VARCHANYA, *Phys. Status Solidi* **17** (1966) 831.
6. A. R. PATEL, C. C. DESAI, *J. Phys. D. Appl. Phys.* **3** (1970) 1645.
7. C. L. SARAF, PhD thesis, Maharaja Sayajirao University of Baroda, Baroda (1971).
8. R. T. SHAH, PhD thesis, Maharaja Sayajirao University of Baroda, Baroda (1976).
9. S. B. TRIVEDI, PhD Thesis, Maharaja Sayajirao University of Baroda, Baroda (1977).
10. A. R. PATEL and S. K. ARORA, *J. Mater. Sci.* **12** (1977) 2124.
11. K. S. RAJU, *Pramana* **8** (1977) 266.
12. A. R. PATEL and S.K. ARORA, *Kristall Technik.* **13** (1978) 1445.
13. M. L. RAO and V. HARIBABU, *J. Mater. Sci.* **16** (1978) 821.
14. U. V. SUBBA RAO and V. HARIBABU, *Pramana* **11** (1978) 149.
15. J. R. PANDYA and C. T. ACHAARYA, *Proc. Nat. Phys. Solid State Phys. Symp.* **21C** (1978) 193.
16. K. N. REDDY, M. L. RAO and V. HARIBABU, *Ind. J. Pure Appl. Phys.* **17** (1979) 806.
17. K. J. PRATAP and V. HARIBABU, *Bull. Mater. Sci.* **2** (1980) 43.
18. U. V. SUBBA RAO and V. HARIBABU, *Ind. J. Pure. Phys.* **54A** (1980) 147.
19. D. W. JOHNSON Jr., E. M VOGEL and B. B. GHATE, in "Proceedings of the Third International Conference on Ferrites", ICF3, Kyoto, Japan, edited by Hiroshi Watanabe (CAP J, Sept.–Oct., 1980) p. 285.
20. V. P. BHATT and C. F. DESAI, *Bull. Mater. Sci.* **4** (1982) 23.
21. L. J. BHAGIA, PhD thesis Maharaja Sayajirao University of Baroda, Baroda (1982).
22. K. NIHARA and T. HIRAI, *J. Less-Common Metals Lett.* **92** (1983) L 15.
23. J. R. PANDYA, L.J. BHAGIA and A. J. SHAH, *Bull. Mater. Sci.* **5** (1983) 79.
24. S. K. ARORA and N. M. BATRA, personal communication (1984).
25. J. R. PANDYA and L. J. BHAGIA, *Ind. J. Pure Appl. Phys.* **22** (1984) 439.
26. R. C. SHAH, PhD thesis, Maharaja Sayajirao University of Baroda, Baroda (1984).
27. P. N. KOTRU, K. K. RAINA, S. K. KACHROO and B. M. WANKLYN, *J. Mater. Sci.* **19** (1984) 2582.
28. B. VENGATESAN, N. KANNIAH and P. RAMASAMY, *J. Mater. Sci. Lett.* **5** (1986) 987.
29. P. N. KOTRU, A. K. RAZDAN and B. M. WANKLYN, *J. Mater. Sci.* **24** (1989) 793.
30. P. N. KOTRU, SUSHMA BHATT and K. K. RAINA, *J. Mater. Sci. Lett.* **8** (1989) 587.
31. ROMESH KUMAR BISHAMBER NATH MARWAHA, PhD thesis, University Saurashtra, Rajkot (1990).
32. F. KICK, "Das Gesetzder, proportionalen widerstande Und Science anwendung" Felix, Leipzig (1885).
33. E. M. ONITSCH, *Mikroskopie* **2** (1947) 131.
34. C. A. BROOKES, in "Science of Hard Materials", edited by R. K. Vishwandham, D. J. Rowoliffe and J. Gurland (Plenum, New York).
35. C. HAYS and E. G. KENDALL, *Metallogr.* **6** (1973) 275.
36. F. W. DANIEL, C. G. DUNN, *Trans. ASM* **41** (1949) 419.
37. P. G. PARTRIDGE and E. ROBERTS, *J. Inst. Metals* **91** (1962) 159.
38. R. P. BURNAND, PhD dissertation, Exeter University (1974).
39. C. A. BROOKES, J. B. O'NEILL and B. A. W. REDFERN, *Proc. R. Soc.* Lond. **A322** (1971).
40. O. O. ADEYVOVE and T. F. PAGE, *J. Mater. Sci.* **11** (1976) 981.
41. D. Y. WATTS and A. F. WILLOUGHBY *J. Appl. Phys.* **56** (1984) 1859.
42. *Idem*, Mater. Lett. **2** (1984) 355.
43. D. V. GITSUE M. P. DYNTU, S. A. SUPOSTAT and A. G. CHEBAN, *Inorg. Mater. (USA)* **14** (1978) 1207.
44. E. M. LEVIN, R. S. ROTH and J. B. MARTIN, *Am. Mineral.* **46** (1961).
45. R. W. G. WYCKOFF, "Crystal Structures" (Wiley, New York, 1964).
46. V. M. GOLDSCHMIDT and H. HAUPTMAN, *Nachr. Ges. Wiss. Gottinges Math Phys. Kl.* **53** (1932).
47. P. N. KOTRU and B. M. WANKLYN, *J. Mater. Sci. Lett.* **14** (1979) 755.
48. B. R. LAWN, B. J. HOCKEY and H. RICHTER, *J. Microsc.* **173** (1983) 295.
49. T. P. DABBS, C. J. FAIRBANKS and B. R. LAWN, "Methods for assessing the structural reliability of brittle materials", edited by Freiman and Hudson, ASTM STP 844 (American Society for Testing and Materials, Philadelphia, PA, 1984).
50. W. BISCHOF and B. WENDEROFF, *Arch. Eisenhuttenw.* **15** (1941–42) 497.
51. E. B. BERGSMAN, "The Micro-hardness Tester" (Victor pettersons, Bokindustriaktiebolag, Stockholm, 1945).
52. D. R. TATE, *Trans. ASM* **35** (1945) 374.
53. N. W. THIBAULT and N. L. NYGUIST *ibid.* **38** (1947) 271.
54. L. P. TAROSOV and W. W. THIBAULT, *ibid.* **38** (1947) 331.
55. R. MITSCHE and E. M. ONITSCH, *Mikroskopie* **3** (1948) 257.
56. R. P. CAMPBELL, Q. HENDERSON and M. R. DONLEAVY, *Trans. ASM* **40** (1948) 954.
57. W. ROSTOKER, *J. Inst. Metals* **77** (1950) 175.
58. A. R. G. BROWN and E. INESON, *J. Iron Steel Inst.* **169** (1951) 376.
59. E. D. BERNHARDT, *Z. Metallkde* **33** (1951) 135.
60. R. SCHULZE, *Feinwerktechnik* **55** (1951) 190.
61. H. BUCKLE, *Metall. Rev.* **4** (1959) 13.
62. J. D. J. ROSS, PhD dissertation, University of Exeter (1984).
63. H. O. 'NEILL, *J. Inst. Metals* **30** (1923) 299.
64. L. B. PFEIL, "The effect of cold work on the structure and hardness of single iron crystals and the changes produced by subsequent annealing", Carnegie Memoires, Iron and Steel Institute, Vol. 16 (1927) p. 153.
65. H. WINCHELL, *Am. Mineral.* **30** (1945) 583.
66. H. BUCKLE, *Rev. Metall.* **48** (1951) 957.
67. B. R. LAWN and D. B. MARSHALL, *J. Am. Ceram. Soc.* **62** (1979) 347.
68. R. W. RICE, in "The Science of hardness Testing and its Research application", edited by J. J. Westbrook and H. Conrad (ASM, Metals Park, OH, 1973) p. 117.
69. J. LANKFORD, *J. Mater. Sci.* **12** (1977) 791.

*Received 20 August 1992*
*and accepted 10 January 1994*